

# Innate Immune Homeostasis by the Homeobox Gene *Caudal* and Commensal-Gut Mutualism in *Drosophila*

Ji-Hwan Ryu,<sup>1\*</sup> Sung-Hee Kim,<sup>1\*</sup> Hyo-Young Lee,<sup>1,2</sup> Jin Young Bai,<sup>1</sup> Young-Do Nam,<sup>3</sup> Jin-Woo Bae,<sup>3</sup> Dong Gun Lee,<sup>4</sup> Seung Chul Shin,<sup>1,5</sup> Eun-Mi Ha,<sup>1</sup> Won-Jae Lee<sup>1†</sup>

Although commensalism with gut microbiota exists in all metazoans, the host factors that maintain this homeostatic relationship remain largely unknown. We show that the intestinal homeobox gene *Caudal* regulates the commensal-gut mutualism by repressing nuclear factor kappa B–dependent antimicrobial peptide genes. Inhibition of *Caudal* expression in flies via RNA interference led to overexpression of antimicrobial peptides, which in turn altered the commensal population within the intestine. In particular, the dominance of one gut microbe, *Gluconobacter* sp. strain EW707, eventually led to gut cell apoptosis and host mortality. However, restoration of a healthy microbiota community and normal host survival in the *Caudal-RNAi* flies was achieved by reintroduction of the *Caudal* gene. These results reveal that a specific genetic deficiency within a host can profoundly influence the gut commensal microbial community and host physiology.

The mucosal epithelia of all metazoans, such as those found in the gastrointestinal tract, are in intimate contact with a large number of commensal microbiota (1). As a consequence, commensal bacteria are known to influence many aspects of the host gut physiology, including innate immunity, development, and homeostasis (2–7). However, the lack of a genetically amenable animal model has limited in-depth analyses of gut-microbe interactions in vivo.

Recent studies have shown that the *Drosophila* gut activates host antimicrobial defense through the production of microbicidal reactive oxygen species (ROS) and antimicrobial peptides (AMPs) (8–11). During most gut-pathogen interactions, intestinal redox homeostasis, mediated via infection-induced ROS generation by the dual oxidase enzyme and subsequent ROS elimination by immune-regulated catalase, is critical for host survival (8, 9). The direct contact between gut epithelia and ingested pathogens also activates the immune deficiency (IMD) pathway and subsequent nuclear localization of the p105-like NF- $\kappa$ B, Relish, which in turn leads to de novo synthesis of diverse immune effectors: AMPs and immunosuppressive enzymes such as the peptidoglycan recognition proteins PGRP-SC and PGRP-LB (10, 12–16). Although pathogen-initiated gut im-

munity is fairly well documented in *Drosophila* (8–10, 14, 16, 17), the molecular interaction between commensals and the *Drosophila* gut is poorly understood.

**Role of gut commensal microbiota in the IMD-Relish pathway.** To investigate the molecular mechanism for commensal-gut interactions, we first asked whether the commensal microbiota could elicit host gut immune responses. We produced germ-free wild-type (GF<sup>WT</sup>) and conventionally reared wild-type (CR<sup>WT</sup>) animals (fig. S1) to enable examination of the gut IMD-Relish pathway potential in the absence or presence of commensals. A large amount of the nuclear-translocated active form of Relish was detected in the intestine cells in the presence of commensals (CR<sup>WT</sup> flies) and was even more pronounced after gut infection with the *Drosophila* pathogen *Erwinia carotovora carotovora-15* (*Ecc15*) (Fig. 1A).

The well-characterized constitutive nuclear localization of Relish in the intestines of CR<sup>WT</sup> flies was almost completely abolished in the absence of commensals in GF<sup>WT</sup> or in antibiotics-treated CR<sup>WT</sup> flies. Similarly, it was not seen in flies carrying a mutation in the IMD-Relish pathway (CR<sup>Dredd</sup> flies) (Fig. 1A). The expression levels of Relish-dependent immunosuppressive enzymes such as PGRP-SC and PGRP-LB (12, 13) were significantly higher in the guts of CR<sup>WT</sup> flies than in the guts of GF<sup>WT</sup> or CR<sup>Dredd</sup> flies (Fig. 1B), which confirms that the IMD-Relish pathway was activated by commensals under normal gut conditions. However, the Relish-dependent immune effector molecules, such as AMP genes including *Cecropin* (*Cec*) and *Diptericin* (*Dpt*), were largely silenced in the CR<sup>WT</sup> gut despite chronic Relish activation. Similarly, no significant difference in AMP expression levels was observed between the GF<sup>WT</sup> and CR<sup>WT</sup> midguts (Fig. 1B).

Taken together, these results indicate that although commensal organisms of the gut can chronically induce a high level of local IMD–NF- $\kappa$ B pathway activation, only a subset of target genes (notably excluding AMP genes) are activated.

**Role of *Caudal* in gut AMP repression.** We next investigated the potential mechanisms of repression of the gut AMP genes to determine how the selective silencing toward commensals might occur. Currently, the cis-regulatory elements controlling epithelial AMP gene expression are poorly understood. It is known, however, that the  $\kappa$ B elements in the promoter regions responsible for nuclear factor kappa B (NF- $\kappa$ B)–Relish binding are essential for inducing epithelial AMP expression (14–16), whereas the CDREs, responsive elements for the homeobox transcription factor *Caudal* (*Cad*) responsible for *Cad* binding, are found to be critical for constitutive AMP expression in certain types of epithelia, such as salivary glands and the ejaculatory duct (18). The homeobox transcription factor *Cad* was originally identified on the basis of its regulatory role in the anteroposterior body axis formation of the *Drosophila* embryo (19, 20). Because *Cad* expression in postembryonic life is known to be mostly restricted to the intestine (19) (fig. S2), we analyzed the contribution of CDREs to gut AMP gene expression in vivo. To accomplish this, we used green fluorescent protein (GFP) reporter–expressing transgenic flies carrying a *Cec* promoter in which the CDREs were mutated (*Cec*<sup>CDRE-mut</sup>-GFP) and compared GFP expression with that of transgenic flies carrying the wild-type promoters fused to GFP (*Cec*-GFP) (Fig. 1C). We were unable to detect any *Cec* reporter activity in the midgut of *Cec*-GFP flies under normal conditions (Fig. 1C). Interestingly, however, *Cec*<sup>CDRE-mut</sup>-GFP flies were found to exhibit high constitutive expression of *Cec* reporter activity in the posterior midgut and the proventriculus in the absence of oral infection (Fig. 1C).

To test whether *Cad* was involved in the negative regulation of *Cec* expression through CDREs, we generated transgenic flies that carried the *UAS-Cad-RNAi* construct to mimic the loss of function (fig. S3) via RNA interference (RNAi). A spontaneous activation of all tested AMPs was observed in the gut of CR<sup>Cad-RNAi</sup> flies under conventional conditions without microbial infection, which was not the case in the control flies (Fig. 1D). Furthermore, similar AMP depression was also observed in *Cad-RNAi* flies with different GAL4 drivers (fig. S4). The role of *Cad* as a repressor was further confirmed by a strong expression of *Dpt* reporter activity observed in the gut of CR<sup>Cad-RNAi</sup> flies carrying the *Dpt-LacZ* reporter (fig. S5). *Cad*-dependent AMP repression is highly tissue-specific because no AMP depression was observed in the fat body of CR<sup>Cad-RNAi</sup> flies (Fig. 1D). Introduction of *Cad-RNAi* had no effect on the expression of PGRP-SC and PGRP-LB (Fig. 1D), which indicates that any repressive role of *Cad* is restricted to a distinct

<sup>1</sup>Division of Molecular Life Science, Ewha Woman's University and National Creative Research Initiative Center for Symbiosystem, Seoul 120-750, South Korea. <sup>2</sup>Laboratoire de BBMI, Institut Pasteur, Paris 75724, France. <sup>3</sup>Biological Resource Center, Korea Research Institute of Bioscience and Biotechnology, Daejeon 305-806, South Korea. <sup>4</sup>School of Life Science and Biotechnology, Kyungpook National University, Daegu 702-701, South Korea. <sup>5</sup>Brain Korea 21 Program, Yonsei University College of Medicine, CPO Box 8044, Seoul 120-752, South Korea.

\*These authors contributed equally to this work.

†To whom correspondence should be addressed. E-mail: lwj@ewha.ac.kr

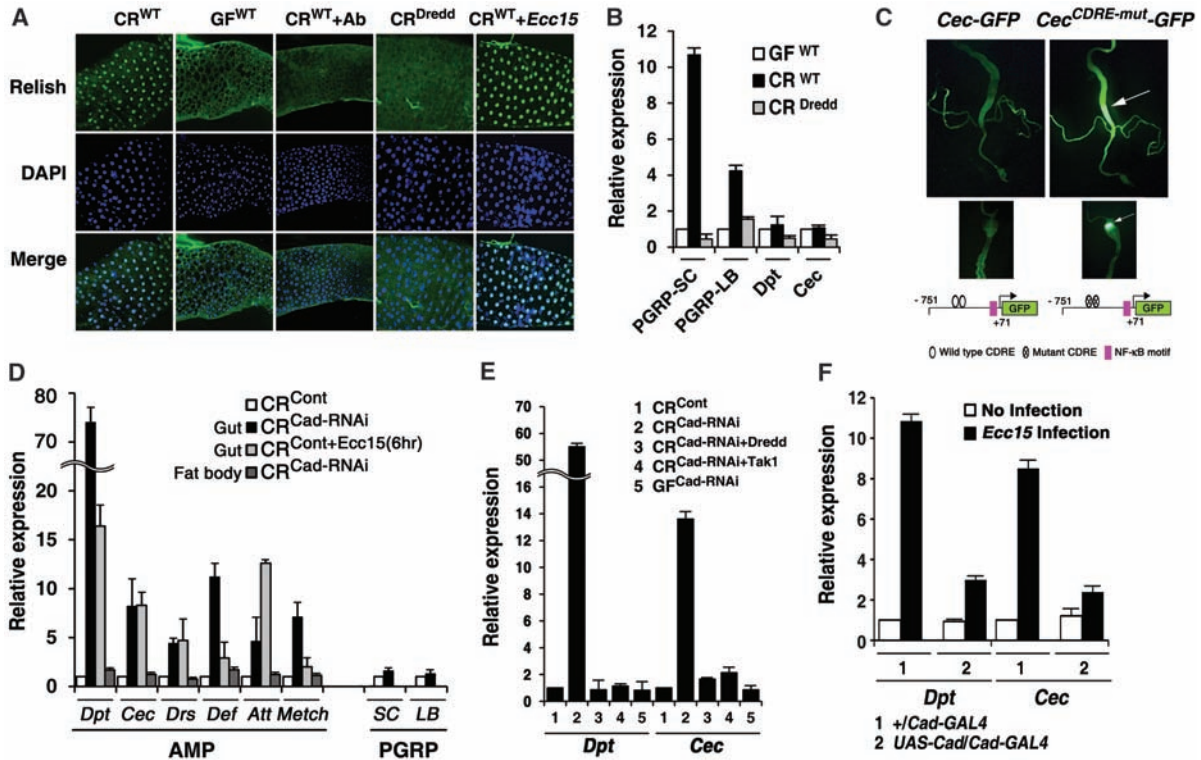


**Fig. 1.** Caudal acts as a gut-specific repressor for NF- $\kappa$ B-dependent AMP genes. (A) Nuclear-translocated active form of Relish (antibody to Relish, green) in posterior midgut (5- or 10-day-old flies). CR<sup>WT</sup>, conventionally reared wild-type flies; GF<sup>WT</sup>, germ-free wild-type flies; CR<sup>WT</sup> + Ab, antibiotics-treated CR<sup>WT</sup> flies as described in fig. S1; CR<sup>Dredd</sup>, conventionally reared *Dredd* mutant flies; CR<sup>WT</sup> + *Ecc15*, natural gut infection with *Ecc15*. Nuclear staining was performed with 4',6'-diamidino-2-phenylindole (DAPI). (B) Quantitative real-time PCR analysis of PGRP-SC, PGRP-LB, Dipterin (Dpt), and Cecropin (Cec) using dissected posterior midguts (without malpighian tubules) of 5-day-old flies. The target gene expression level in the tissues of GF<sup>WT</sup> flies was taken arbitrarily as 1. (C) CDREs are required for the repression of *Cec* expression (indicated by arrow) in the posterior midgut (upper panel) and the proventriculus (lower panel). A schematic diagram of the *Cec* promoter is also shown. (D) Quantitative real-time PCR analysis using posterior

midguts or fat body. Genotypes of flies: CR<sup>Cont</sup> (*c729-GAL4/+*) and CR<sup>Cad-RNAi</sup> (*c729-GAL4/+; UAS-Cad-RNAi/+*). The target gene expression level in the gut or fat body of CR<sup>Cont</sup> flies was taken arbitrarily as 1. Dpt, Dipterin; Cec, Cecropin; Drs, Drosomycin; Def, Defensin; Att, Attacin; Metch, Metchnikowin. (E) Quantitative real-time PCR analysis. Genotypes of flies (5-day-old GF or CR): Cont (*c729-GAL4/+*); Cad-RNAi (*c729-GAL4/+; UAS-Cad-RNAi/+*); Cad-RNAi + *Dredd* (*Dredd<sup>B118</sup>; c729-GAL4/+; UAS-Cad-RNAi/+*); Cad-RNAi + TAK1 (*TAK1; c729-GAL4/+; UAS-Cad-RNAi/+*); GF-Cad-RNAi. The target gene expression level in the CR<sup>Cont</sup> gut was taken arbitrarily as 1. (F) Overexpression of *Cad* can abolish infection-induced AMP expression. The target gene expression level in uninfected control gut was taken arbitrarily as 1. Natural gut infection for 6 hours with *Ecc15* in (A), (D), and (F) was performed as described in (21); relative expression levels in (B), (D), (E), and (F) are expressed as means  $\pm$  SD ( $P < 0.05$ ) of three different experiments.

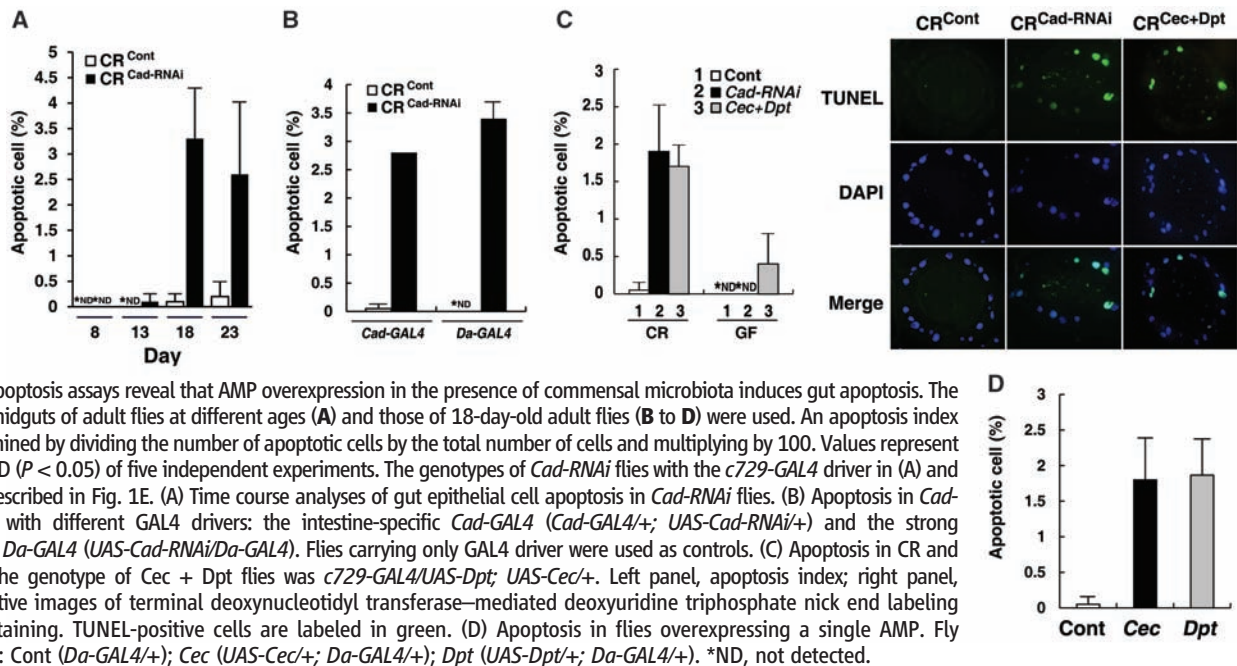


**Fig. 2.** Apoptosis assays reveal that AMP overexpression in the presence of commensal microbiota induces gut apoptosis. The posterior midguts of adult flies at different ages (A) and those of 18-day-old adult flies (B to D) were used. An apoptosis index was determined by dividing the number of apoptotic cells by the total number of cells and multiplying by 100. Values represent means  $\pm$  SD ( $P < 0.05$ ) of five independent experiments. The genotypes of *Cad-RNAi* flies with the *c729-GAL4* driver in (A) and (C) were described in Fig. 1E. (A) Time course analyses of gut epithelial cell apoptosis in *Cad-RNAi* flies. (B) Apoptosis in *Cad-RNAi* flies with different GAL4 drivers: the intestine-specific *Cad-GAL4* (*Cad-GAL4/+; UAS-Cad-RNAi/+*) and the strong ubiquitous *Da-GAL4* (*UAS-Cad-RNAi/Da-GAL4*). Flies carrying only GAL4 driver were used as controls. (C) Apoptosis in CR and GF flies. The genotype of *Cec* + *Dpt* flies was *c729-GAL4/UAS-Dpt; UAS-Cec/+*. Left panel, apoptosis index; right panel, representative images of terminal deoxynucleotidyl transferase-mediated deoxyuridine triphosphate nick end labeling (TUNEL) staining. TUNEL-positive cells are labeled in green. (D) Apoptosis in flies overexpressing a single AMP. Fly genotypes: Cont (*Da-GAL4/+*); *Cec* (*UAS-Cec/+; Da-GAL4/+*); *Dpt* (*UAS-Dpt/+; Da-GAL4/+*). \*ND, not detected.

subset of NF- $\kappa$ B-dependent genes such as AMPs. When we examined *Cad-RNAi*-induced AMP derepression in the IMD-Relish pathway mutant genetic backgrounds (CR<sup>*Cad-RNAi* + Dredd</sup> or CR<sup>*Cad-RNAi* + TAK1</sup> flies) or in the absence of commensals (GF<sup>*Cad-RNAi*</sup> flies), the high level of AMP derepression was completely abolished (Fig. 1E).

These data show that *Cad* acts as a gut-specific transcriptional repressor exerting its antagonistic role in commensal-induced NF- $\kappa$ B-dependent AMP induction. Furthermore, the overexpression of *Cad* in the gut could abolish the infection-induced AMP expression (Fig. 1F).

Thus, it is likely that a dynamic equilibrium between *Cad* and Relish is one of the major mechanistic aspects determining the selective deployment of gut IMD-AMP pathway potential (21) (Fig. 1 and fig. S6). Because AMPs have a microbicidal effect against a broad spectrum of microorganisms, *Cad*-mediated AMP repression is likely required for establishing an optimal environment for the commensal microbiota.

**Role of *Cad* in gut homeostasis.** Several recent lines of evidence suggest that deregulation of the intestinal NF- $\kappa$ B pathway may be relevant to the etiology and pathology of many important diseases, including inflammatory bowel diseases

(IBDs) (22–29). Given that IBDs typically involve apoptosis of intestinal cells, we examined whether cell death might be occurring in the gut of *Cad-RNAi* flies. Time-course analyses with adult flies showed that gut epithelial cell apoptosis was detected in *Cad-RNAi* flies at day 18, but not in control flies of the same age (Fig. 2A). Cell death was also observed in the intestines of CR<sup>*Cad-RNAi*</sup> flies with different GAL4 drivers: *c729-GAL4*, *Cad-GAL4*, and *Da-GAL4* (Fig. 2, A and B). Interestingly, gut epithelial cell apoptosis was abolished in the GF<sup>*Cad-RNAi*</sup> gut (Fig. 2C), which suggests the involvement of commensal organisms in *Cad-RNAi*-mediated gut pathology. To determine whether the high apoptosis level seen in the *Cad-RNAi* gut was due to secondary effects of AMP hyperactivation, we overexpressed two AMP genes (*Cec* and *Dpt*) to mimic the *Cad-RNAi* genotype. AMP overexpression in CR flies (CR<sup>*Cec+Dpt*</sup>) was sufficient to induce a high level of gut epithelial cell apoptosis (Fig. 2C). This was not the case in the absence of commensal microbiota (GF<sup>*Cec+Dpt*</sup>) (Fig. 2C). When we overexpressed only a single AMP (*Cec* or *Dpt*) in CR flies (CR<sup>*Cec*</sup> or CR<sup>*Dpt*</sup>), similar gut epithelial cell apoptosis could be also observed (Fig. 2D). Overall, these in vivo results show that gut AMP overexpression in the presence but not in the absence of gut commensal microbes is sufficient to cause gut pathology.

**Role of *Cad* in the gut commensal community structure.** Because constitutive production of AMPs in the guts of *Cad-RNAi* flies likely affects the ecosystem of normal commensals, we next determined the dominant commensal species in the midgut of control (CR<sup>Cont</sup>) and *Cad-RNAi* (CR<sup>*Cad-RNAi*</sup>) flies. In wild-type flies, five commensal species dominate: *Lactobacillus plantarum* (*LP*), *Lactobacillus brevis* (*LB*), *Acetobacter pomorum* (*AP*), and two novel strains: *Gluconobacter* sp. strain EW707 (*G707*), and a bacterium in the family *Acetobacteraceae*, strain EW911 (*A911*) (21) (figs. S7 to S9 and table S1). All of these commensal bacteria, but not other bacteria such as *Ecc15* and *Escherichia coli*, could persist in the gut, demonstrating their competences as commensal bacteria (Fig. 3A). Real-time polymerase chain reaction (PCR)-based quantitative analyses of each commensal (21) (figs. S9 to S11) clearly revealed that the commensal community structure of the *Cad-RNAi* flies differed from that of the control flies (Fig. 3B). Three bacteria—*AP*, *LP*, and *LB*—were commonly dominant in the gut of both control and *Cad-RNAi* flies (Fig. 3B). However, *A911* [a dominant commensal member in controls,  $\sim 1.4 \times 10^5$  colony-forming units (CFUs) per gut] was markedly diminished and maintained at a very low level in the *Cad-RNAi* gut ( $\sim 900$  CFUs per gut), whereas *G707* (a minor commensal member in the control gut,  $\sim 800$  CFUs per gut) emerged as a dominant commensal in the *Cad-RNAi* gut ( $\sim 1.7 \times 10^4$  CFUs per gut) (Fig. 3B). Time-course analyses with *Cad-RNAi* flies showed that loss of *A911* was visible from as

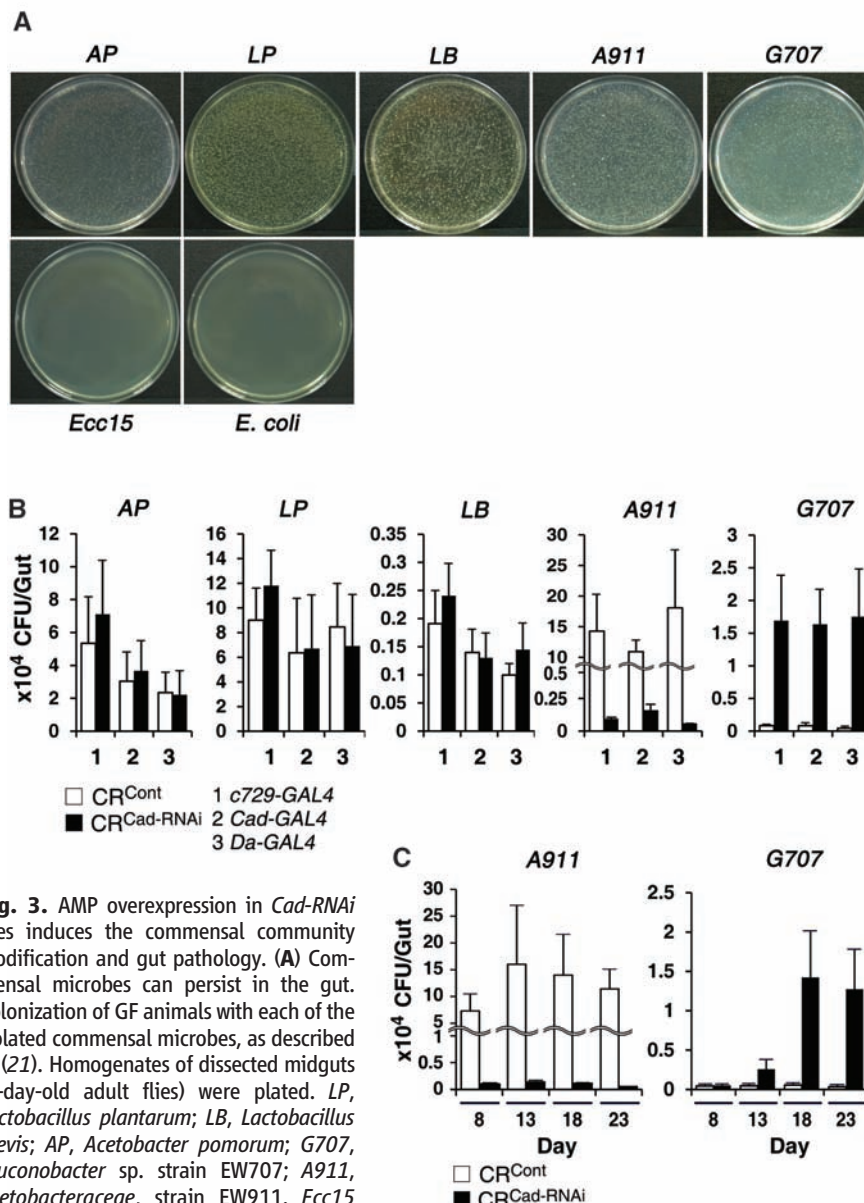


**Fig. 3.** AMP overexpression in *Cad-RNAi* flies induces the commensal community modification and gut pathology. (A) Commensal microbes can persist in the gut. Colonization of GF animals with each of the isolated commensal microbes, as described in (21). Homogenates of dissected midguts (8-day-old adult flies) were plated. *LP*, *Lactobacillus plantarum*; *LB*, *Lactobacillus brevis*; *AP*, *Acetobacter pomorum*; *G707*, *Gluconobacter* sp. strain EW707; *A911*, *Acetobacteraceae*, strain EW911. *Ecc15* and *E. coli* were also used as noncommensal microbes. (B and C) Real-time PCR-based analysis to quantify the number of each commensal microbe in the posterior midguts. Values represent means  $\pm$  SD ( $P < 0.05$ ) of three independent experiments. The genotypes of *Cad-RNAi* flies with the *c729-GAL4* driver were described in Fig. 1E. *Cad-RNAi* flies with *Cad-GAL4* or *Da-GAL4* were described in Fig. 2B. The posterior midguts of 18-day-old adult flies (B) and those of adult flies at different ages (C) were used.

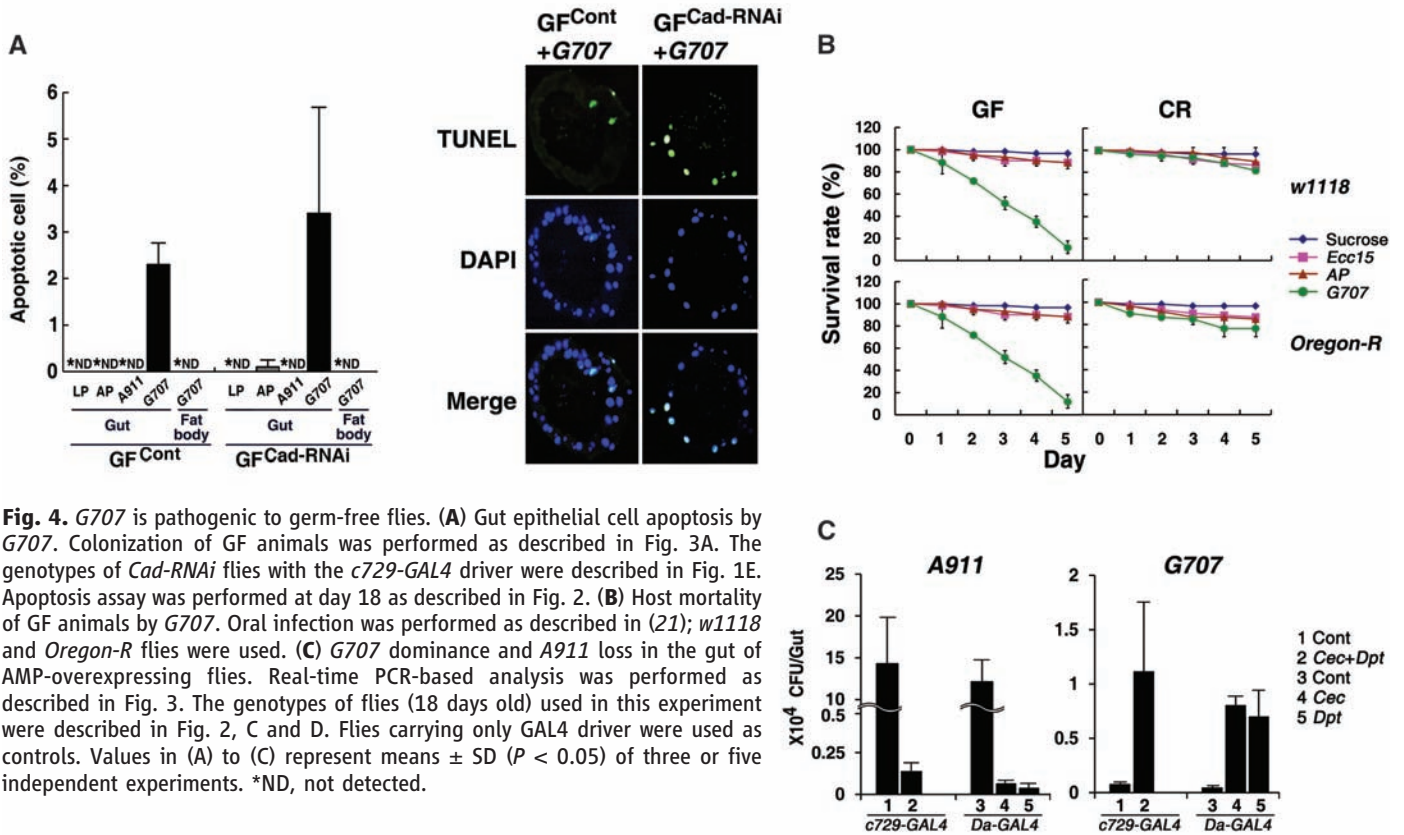


**Fig. 4.** *G707* is pathogenic to germ-free flies. (A) Gut epithelial cell apoptosis by *G707*. Colonization of GF animals was performed as described in Fig. 3A. The genotypes of *Cad-RNAi* flies with the *c729-GAL4* driver were described in Fig. 1E. Apoptosis assay was performed at day 18 as described in Fig. 2. (B) Host mortality of GF animals by *G707*. Oral infection was performed as described in (21); *w1118* and *Oregon-R* flies were used. (C) *G707* dominance and *A911* loss in the gut of AMP-overexpressing flies. Real-time PCR-based analysis was performed as described in Fig. 3. The genotypes of flies (18 days old) used in this experiment were described in Fig. 2, C and D. Flies carrying only GAL4 driver were used as controls. Values in (A) to (C) represent means  $\pm$  SD ( $P < 0.05$ ) of three or five independent experiments. \*ND, not detected.

**Table 1.** In vitro antibacterial assay using synthetic Cec A1, performed as described in (21). The minimal Cec A1 concentration that prevented the growth of a given test organism was determined and was defined as the minimum inhibitory concentration (MIC).

Gram-positive bacteria		Gram-negative bacteria			
<i>LP</i>	<i>LB</i>	<i>AP</i>	<i>G707</i>	<i>A911</i>	<i>E. coli</i> *
10 to 20	10 to 20	2.5	2.5	0.625	1.25

\**E. coli* ATCC 25922.

early as day 8, whereas dominance of *G707* started at day 13 and reached the maximum level at day 18 (Fig. 3C). Given the high apoptosis levels in the gut epithelial cells of GF<sup>Cont</sup> flies fed on the homogenates of the CR<sup>Cad-RNAi</sup> gut, but not on homogenates of the CR<sup>Cont</sup> gut (fig. S12), we reasoned that the dominant commensals in the *Cad-RNAi* gut, such as *G707*, may be involved in the gut pathology.

To validate this hypothesis, we introduced each of the isolated commensal bacteria into GF<sup>Cont</sup> or GF<sup>Cad-RNAi</sup> embryos and maintained these bacteria until the adult stage to generate monoassociated flies. High gut epithelial cell apoptosis was observed in all of the GF flies (GF<sup>Cont</sup> or GF<sup>Cad-RNAi</sup>) when the single organism was *G707* (Fig. 4A), but not when the single organism was one of the other commensal organisms (*LP*, *AP*, or *A911*) (Fig. 4A). Additionally, *G707* did not induce the apoptosis in the fat body (Fig. 4A), and *G707* was pathogenic to the host when GF flies were subjected to gut infection with

*G707* (Fig. 4B). These results show that *G707* is indeed pathogenic in a gut-specific manner when allowed to become the dominant gut microbe.

To further confirm that reorganization of the gut microbiota composition seen in the *Cad-RNAi* flies was due to the constitutive overexpression of microbicidal AMPs, we tested whether the artificial shift of gut microbiota composition could occur as a result of overexpression of AMPs. We found that overexpression of *Cec* and *Dpt* (CR<sup>Cec+Dpt</sup>) was sufficient to induce the modification of commensal community (i.e., *G707* dominance and a loss of *A911*), as in the case of the *Cad-RNAi* guts (Fig. 4C). Similar results could also be observed when we overexpressed only a single AMP (CR<sup>Cec</sup> or CR<sup>Dpt</sup>) (Fig. 4C). To confirm that the loss of *A911* was due to the high sensitivity of this strain to AMP, we performed an in vitro antibacterial test with synthetic Cec A1 and determined the minimum inhibitory concentration (21). The result showed that *A911* was highly susceptible to

low concentrations of synthetic Cec A1, whereas all other commensals as well as *G707* exhibited relatively high resistance to Cec A1 (Table 1). Thus, we conclude that gut AMP overexpression in *Cad-RNAi* flies acts as a distinct selection pressure on different commensal microbes, resulting in modification of the commensal community structure and pathogenic conditions in the gut.

**Role of the normal commensal community in gut homeostasis.** Because *G707* is normally present at a very low level in the wild-type commensal community, we investigated whether the normal wild-type commensal community structure could antagonize the dominance of *G707*. To accomplish this, we introduced *G707* by oral feeding into the gut of either GF<sup>WT</sup> or CR<sup>WT</sup> flies and then examined its persistence. The results indicated that *G707* bacteria could persist in the absence of other commensal organisms in GF<sup>WT</sup> flies but disappeared rapidly and were maintained at a low level in the presence of the normal commensal community in CR<sup>WT</sup> flies (Fig. 5A). Consistent with these results, we observed a high-level gut epithelial cell apoptosis in the *G707*-challenged GF<sup>WT</sup> flies, but not in the *G707*-challenged CR<sup>WT</sup> flies (Fig. 5A), which demonstrates the role of normal commensal community structure in gut homeostasis by maintaining *G707* at a low level.

Given the numerical inferiority of *A911* in *G707*-dominant gut environments, we investigated whether the presence of *A911* was suf-

ficient to suppress *G707* dominance in the gut. To accomplish this, we generated monoassociated flies by introducing isolated *A911* into GF<sup>WT</sup> embryos and maintaining this presence until the adult stage. When *G707* was introduced into these monoassociated flies through oral feeding, the *G707* bacteria rapidly decreased to a low level in the presence of *A911*, whereas a high initial *G707* level was able to persist in the absence of *A911* (in the case of GF<sup>WT</sup> flies) (Fig. 5A). After *G707* introduction, a high apoptosis index was observed in the gut of the GF<sup>WT</sup> flies, but not in the gut of *A911*-monoassociated flies (Fig. 5A). This result shows that the presence of *A911* is sufficient to prevent *G707* dominance, and that the loss of *A911* in the AMP-overexpressing genotype flies (such as *Cad-RNAi* flies or *Cec-* or *Dpt*-overexpressing flies) is likely to be responsible for *G707* dominance.

Taken together, these results reveal that *Cad* acts as a critical host factor that maintains the immune homeostasis responsible for preservation of the normal commensal community structure. Failure of the balanced regulation of AMP, as in the case of *Cad-RNAi* flies, can act as a novel selection pressure leading to modification of the gut commensal structure. Because *G707* is a highly pathogenic organism (Fig. 4, A and B), the *G707*-dominating host genotype acts as an initial cause of gut apoptosis, whereas the dominance of *G707* acts as a direct cause of gut apoptosis.

**Role of *Cad* in host physiology.** The apoptosis of gut cells seen in *Cad-RNAi* flies with different GAL4 drivers was accompanied by elevated mortality (Fig. 5E and figs. S13 and S14). The high mortality of CR<sup>*Cad-RNAi*</sup> flies was significantly ameliorated in the absence of commensal (GF<sup>*Cad-RNAi*</sup> flies) (Fig. 5E) or in the presence of commensals under the IMD pathway mutant genetic backgrounds (CR<sup>*Cad-RNAi*</sup> + *Dredd*) (fig. S14). The normal survival rate could be also observed in GF<sup>*Cad-RNAi*</sup> flies stably associated with major commensal microbiota (*AP*, *LP*, *LB*, and *A911*) excluding *G707*, which implies the involvement of *G707* in *Cad-RNAi*-mediated host mortality (Fig. 5E). Furthermore, the c-Jun N-terminal kinase pathway and interleukin-1 $\beta$  converting enzyme were shown to be involved in the microbiota-induced gut apoptosis and mortality process of the *Cad-RNAi* flies (fig. S15).

To demonstrate that the initial cause of death in the *Cad-RNAi* flies was the reduced expression of *Cad*, we attempted an in vivo rescue experiment. Restoration of the basal AMP level (Fig. 5B), healthy microbiota community structure (Fig. 5C), reduced apoptosis (Fig. 5D), and normal host survival levels (Fig. 5E) could be achieved in the *Cad-RNAi* flies by genetic reintroduction of *Cad* (CR<sup>*Cad-RNAi*</sup> + *Cad* flies). Taken together, our results show that the intestinal homeobox *Cad* gene is responsible for the delicate immune homeostasis in the microbe-contacting gut tissue, which is essential for preservation of the normal microbiota community, gut homeostasis, and host survival.

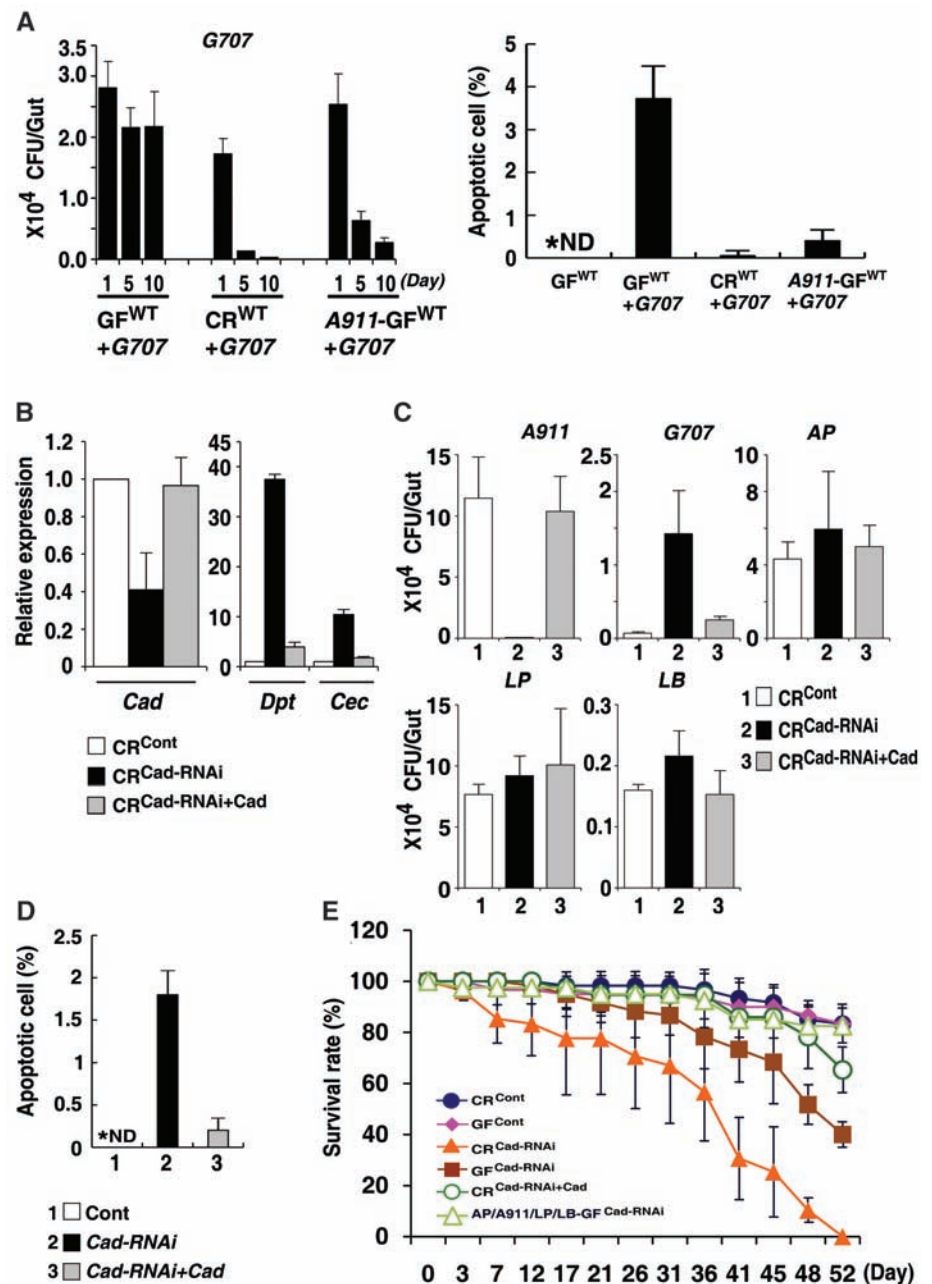


**Fig. 5.** *Cad* is indispensable for immune homeostasis in preserving the indigenous commensal community and host health. (A) Normal commensal community structure is important to suppress *G707* dominance in the gut. Germ-free wild-type flies (GF<sup>WT</sup>), wild-type flies carrying normal commensal microbiota (CR<sup>WT</sup>), and wild-type flies monoassociated with *A911* (A911-GF<sup>WT</sup>) were used. *G707* was introduced to these flies (3 days old) through oral feeding for 48 hours. Left panel: Real-time PCR-based analysis to quantify *G707* in the gut was performed at 1, 5, and 10 days after *G707* feeding. Right panel: Apoptosis assay was performed as described in Fig. 2. Values represent means  $\pm$  SD ( $P < 0.05$ ) of five independent experiments. (B to E) Restoration of basal AMP levels (B), normal commensal community structure (C), reduced apoptosis (D), and normal survival levels (E) could be achieved in the *Cad-RNAi* flies by genetic reintroduction of *Cad*. The posterior midguts of 18-day-old adult flies were used for analyses of commensal community structure and apoptosis. Apoptosis assay was performed as described in Fig. 2. Genotypes of CR flies: Cont (*c729-GAL4/+*); *Cad-RNAi* (*c729-GAL4/+; UAS-Cad-RNAi/+*); *Cad-RNAi* + *Cad* (*c729-GAL4/UAS-Cad; UAS-Cad-RNAi/+*). GF<sup>Cont</sup> and GF<sup>*Cad-RNAi*</sup> flies were also used. AP/A911/LP/LB-GF<sup>*Cad-RNAi*</sup> flies carrying four major commensals (*AP*, *A911*, *LP*, and *LB*, excluding *G707*) were generated by colonizing GF embryos with commensals as described in (21). Values represent means  $\pm$  SD ( $P < 0.05$ ) of three independent experiments. \*ND, not detected.

**Discussion.** The gut epithelia of virtually all organisms have evolved to form a mutually beneficial strategic alliance with microorganisms (6). However, the role of the host factor in gut homeostasis has been largely overlooked, and little information regarding the molecular principles of gut homeostasis established by the interrelationship between the host immunity and commensal microbiota is available. In mammalian gut epithelia, deregulation of the NF- $\kappa$ B and AMP signaling pathways was found to be implicated in the pathogenesis of chronic IBDS (22–29). However, the enormous diversity of the resident microbiota community of the mammalian gut (e.g., 500 to 1000 different species in the human gut) (30) and the genetic complexity of the host immune system make it difficult to clearly establish the molecular links that would clarify the relations among immune genotype, commensal microbiota structure, and disease phenotype at the organism level.

By using a genetically amenable model organism harboring an extremely simple gut commensal structure, we have shown that the commensal microbiota community structure links the defective immune genotype to the gut disease phenotype. Surprisingly, *Drosophila* gut epithelia have evolved an immune strategy by recruiting a developmental master control gene, *Cad*, to maintain appropriate AMP levels for preservation of the normal flora community structure. Defec-

tive regulation of the AMP level, as seen in the case of the *Cad-RNAi* genotype, promotes gut pathology by exerting a selection pressure that favors the dominance of a pathogenic commensal, *G707*, rather than by acting as a direct cause of the disease phenotype. The emergence of a disease-causing commensal organism under an immune-defective genotype indicates the involvement of a microorganism as an origin of chronic inflammation. Further elucidation of the link between the immune genotype-based commensal community structure and host physiology may provide important insights into the causative role of pathogenic commensal microbes in a variety of chronic inflammatory diseases of the commensal-contacting epithelia.

#### References and Notes

1. L. V. Hooper, J. I. Gordon, *Science* **292**, 1115 (2001).
2. T. T. Macdonald, G. Monteleone, *Science* **307**, 1920 (2005).
3. F. Bäckhed, R. E. Ley, J. L. Sonnenburg, D. A. Peterson, J. I. Gordon, *Science* **307**, 1915 (2005).
4. T. A. Koropatnick *et al.*, *Science* **306**, 1186 (2004).
5. P. J. Turnbaugh *et al.*, *Nature* **444**, 1027 (2006).
6. C. Dale, N. A. Moran, *Cell* **126**, 453 (2006).
7. S. Rakoff-Nahoum, J. Paglino, F. Eslami-Varzaneh, S. Edberg, R. Medzhitov, *Cell* **118**, 229 (2004).
8. E.-M. Ha, C.-T. Oh, Y. S. Bae, W.-J. Lee, *Science* **310**, 847 (2005).
9. E. M. Ha *et al.*, *Dev. Cell* **8**, 125 (2005).
10. J. H. Ryu *et al.*, *EMBO J.* **25**, 3693 (2006).
11. B. Lemaitre, J. Hoffmann, *Annu. Rev. Immunol.* **25**, 697 (2007).

12. A. Zaidman-Remy *et al.*, *Immunity* **24**, 463 (2006).
13. V. Bischoff *et al.*, *PLoS Pathog.* **2**, e14 (2006).
14. D. Ferrandon *et al.*, *EMBO J.* **17**, 1217 (1998).
15. T. Onfelt Tingvall, E. Roos, Y. Engstrom, *EMBO Rep.* **2**, 239 (2001).
16. P. Tzou *et al.*, *Immunity* **13**, 737 (2000).
17. N. Vodovar *et al.*, *Proc. Natl. Acad. Sci. U.S.A.* **102**, 11414 (2005).
18. J. H. Ryu *et al.*, *Mol. Cell. Biol.* **24**, 172 (2004).
19. M. Mlodzik, W. J. Gehring, *Cell* **48**, 465 (1987).
20. E. Moreno, G. Morata, *Nature* **400**, 873 (1999).
21. See supporting material on Science Online.
22. M. Karin, T. Lawrence, V. Nizet, *Cell* **124**, 823 (2006).
23. C. Zaph *et al.*, *Nature* **446**, 552 (2007).
24. K. S. Kobayashi *et al.*, *Science* **307**, 731 (2005).
25. S. Maeda *et al.*, *Science* **307**, 734 (2005).
26. A. Nenci *et al.*, *Nature* **446**, 557 (2007).
27. R. J. Xavier, D. K. Podolsky, *Nature* **448**, 427 (2007).
28. H. Xiao *et al.*, *Immunity* **26**, 461 (2007).
29. N. H. Salzman, M. A. Underwood, C. L. Bevins, *Semin. Immunol.* **19**, 70 (2007).
30. P. B. Eckburg *et al.*, *Science* **308**, 1635 (2005); published online 14 April 2005 (10.1126/science.1110591).
31. Supported by the National Creative Research Initiative Program of the Ministry of Science and Technology, Korea.

#### Supporting Online Material

www.sciencemag.org/cgi/content/full/1149357/DC1  
Materials and Methods

SOM Text

Figs. S1 to S15

Table S1

References

17 August 2007; accepted 21 December 2007

Published online 24 January 2008;

10.1126/science.1149357

Include this information when citing this paper.

## REPORTS

# Quantum Phase Extraction in Isospectral Electronic Nanostructures

Christopher R. Moon,<sup>1</sup> Laila S. Mattos,<sup>1</sup> Brian K. Foster,<sup>2</sup> Gabriel Zeltzer,<sup>3</sup> Wonhee Ko,<sup>3</sup> Hari C. Manoharan<sup>1\*</sup>

Quantum phase is not directly observable and is usually determined by interferometric methods. We present a method to map complete electron wave functions, including internal quantum phase information, from measured single-state probability densities. We harness the mathematical discovery of drum-like manifolds bearing different shapes but identical resonances, and construct quantum isospectral nanostructures with matching electronic structure but divergent physical structure. Quantum measurement (scanning tunneling microscopy) of these “quantum drums”—degenerate two-dimensional electron states on the copper(111) surface confined by individually positioned carbon monoxide molecules—reveals that isospectrality provides an extra topological degree of freedom enabling robust quantum state transplantation and phase extraction.

The local structure of wave functions can now be experimentally determined in many materials. However, just as bonding in molecules or conductivity in solids depends not only on the magnitude of the orbital wave functions but also on the phase, the electronic properties and dynamics of nanostructures critically depend on determining both the magnitude and the phase of wave functions. In a

classical system, measuring the phase of a standing wave is trivial, but the internal phase of a quantum wave function  $\psi$  is not an observable; only the probability density  $|\psi|^2$  can be determined from direct measurement. To determine phase, some form of additional information is required.

Recently, quantum phase has been inferred in several experiments, including spectral inter-

fometry of Rydberg wave packets (1) and tomography of molecular orbitals (2). Such experiments are performed on atoms or molecules in the gas phase and require ultrafast measurements of the response of a quantum state to an impinging wave or excitation. In solid-state systems, phase-sensitive measurements have been performed in quantum dots and rings (3) and with computational post-processing of diffraction patterns (4). All of these experiments retrieve the underlying phase differences through interferometry once a reference beam and geometry are defined.

Here, we present a noninterferometric method to map the internal quantum phase of a solitary, time-independent state by harnessing the topological property of isospectrality as the additional degree of freedom. We create a particular pair of geometric shapes with matching spectral properties. We then show that the complete phase information of wave functions in both structures can be experimentally deter-

<sup>1</sup>Department of Physics, Stanford University, Stanford, CA 94305, USA. <sup>2</sup>Department of Electrical Engineering, Stanford University, Stanford, CA 94305, USA. <sup>3</sup>Department of Applied Physics, Stanford University, Stanford, CA 94305, USA.

\*To whom correspondence should be addressed. E-mail: manoharan@stanford.edu